Central Finite Volume Methods Applied in Relativistic Magnetohydrodynamics: Applications in Disks and Jets

Raphael de Oliveira Garcia, Samuel Rocha de Oliveira

Abstract—We have developed a new computer program in Fortran 90, in order to obtain numerical solutions of a system of Relativistic Magnetohydrodynamics partial differential equations with predetermined gravitation (GRMHD), capable of simulating the formation of relativistic jets from the accretion disk of matter up to his ejection. Initially we carried out a study on numerical methods of unidimensional Finite Volume, namely Lax-Friedrichs, Lax-Wendroff, Nessyahu-Tadmor method and Godunov methods dependent on Riemann problems, applied to equations Euler in order to verify their main features and make comparisons among those methods. It was then implemented the method of Finite Volume Centered of Nessyahu-Tadmor, a numerical schemes that has a formulation free and without dimensional separation of Riemann problem solvers, even in two or more spatial dimensions, at this point, already applied in equations GRMHD. Finally, the Nessyahu-Tadmor method was possible to obtain stable numerical solutions - without spurious oscillations or excessive dissipation - from the magnetized accretion disk process in rotation with respect to a central black hole (BH) Schwarzschild and immersed in a magnetosphere, for the ejection of matter in the form of jet over a distance of fourteen times the radius of the BH, a record in terms of astrophysical simulation of this kind. Also in our simulations, we managed to get substructures jets. A great advantage obtained was that, with the our code, we got simulate GRMHD equations in a simple personal computer.

Keywords—Finite Volume Methods, Central Schemes, Fortran 90, Relativistic Astrophysics, Jet.

I. INTRODUCTION

IN recent decades, the applications of numerical methods and computational techniques in simulations of astrophysical systems are becoming increasingly intensified, due to advances obtained in numerical analysis researches, scientific computing, analytical studies, observational and experimental techniques. However, new scenarios, phenomena, properties and characteristics are discovered and detailed collaborating with the understanding of fluid flow in astrophysical processes.

Central compact objects that attract the matter around them, resulting in the formation of relativistic jets, earn highlight for they are large emitters of energy that influence many galactic processes [7]. These phenomena are modeled by the Magnetohydrodynamics equations and General Relativity (GRMHD) [31].

R. O. Garcia and S. R. Oliveira are with the Department of Applied Mathematics, Institute of Mathematics, Statistics and Scientific Computing, University of Campinas, Campinas-SP, 13083-859 Brazil, e-mail: gr.gubim@gmail.com (first author) and samuel@ime.unicamp.br (second author).

Due the complexity of the differential equations system from GRMHD, the computational difficulty of treatment imposed by non-linear character of the equations and by involving phenomena that operate in different orders of magnitudes, the processes of plasma accretion and ejection by the central compact object were initially treated separately [3], [4], [8], [28].

Simulations that consider the accretion process, jet formation and its ejection in the same temporal evolution have been recently researched by Koide [17], Nishikawa [24], McKinney [20], Shibata [16], among others. However, the computational implementations of these phenomena by means of numerical methods still pose challenges because they require much attention on issues involving order of accuracy, discontinuities in the solution of the equations, stability of numerical methods, processing time (CPU time) and memory used.

Another point of difficulty is the moment of transition between the accretion disk and the beginning of the formation of collimated jet formation, because in this situation the quantities involved have abrupt variations characteristic of the phenomenon and an inadequate numerical treatment can add spurious oscillations or excessive numerical dissipation that impair the simulation's performance.

Such difficulties can be perceived by two facts: since the pioneering work of Koide, Shibata and Kudoh (1999) [16] to the present day, researchers still use the Lax-Wendroff method with the following properties: Total Variation Diminishing (TVD) in the time; Artificial Viscosity; *dimensional splitting* and slope limiters to avoid oscillations; and the other fact is that the current codes available in GRMHD don't have the relativistic jets formation modeling problems from the accretion disk to the ejection of matter.

Currently, the main codes used for the GRMHD equations have an emphasis on Godunov methods that need of analytical or approximate Riemann Solvers, with dimensional splitting and slope limiter, even though the equations system have degeneracy of eigenvalues obtained from the Jacobian matrix [1], [5], [6], [9], [10], [12], [22], [29]. This limits the applicability of such methods. Another restrictive issue associated with these methods is the use of dimensional splitting, which aren't recommended for problems whose eigenvalues have large differences in orders of magnitude. These differences occur exactly at the

World Academy of Science, Engineering and Technology
International Journal of Mathematical and Computational Sciences
Vol:9, No:1, 2015

transition that defines the formation of jets.

In this context, the main objective of this work was to develop a new GRMHD code applied to the formation of relativistic jets, able to describe it from the accretion of matter in the form of a disk until the collimated ejection. Featuring a jet by applying central schemes of Finite Volumes without dimensional decomposition, in order to better represent the temporal evolution of astrophysical system with a larger extent than found in the literature [17], [16].

This paper was divided as follows: in Section II we present the basic equations needed for the modeling and simulation of jets formation; in Section III we show numerical methods that were applied on problem in study and also we performed comparisons between the approximate solutions obtained from the schemes applied on the unidimensional Euler equations; in Section IV we have a simulation of relativistic jet formation through the new code developed in Fortran 90, the numerical solutions were obtained through the two-dimensional Nessyahu-Tadmor method and the Euler method of four stages to add terms sources; and in Section V we wrote the conclusions of this work.

II. MODELING OF RELATIVISTIC JETS

A. Fundamental Equations

The equations that provide base to the mathematical modeling of relativistic jets come from the relativistic magnetohydrodynamics (GRMHD), which consists of relativistic balance laws of mass, momentum and energy, coupled with the Electromagnetism [31],

$$\nabla_\mu(\rho U^\nu) = 0 \, , \qquad (1)$$
$$\nabla_\mu T_g^{\mu\nu} = 0 \, , \qquad (2)$$
$$\partial_\mu F_{\nu\lambda} + \partial_\nu F_{\lambda\mu} + \partial_\lambda F_{\mu\nu} = 0 \, , \qquad (3)$$
$$\nabla_\mu F^{\mu\nu} = 0 \, , \qquad (4)$$

where U^ν are the components of the four-velocity. The scalars ρ, p and ϵ are the proper density, proper pressure and density of proper total energy

$$\epsilon = \rho c^2 + \frac{p}{\Gamma - 1} \, ,$$

respectively. The constant Γ is related to the specific heat, ∇_ν is covariante derivate. The components of the energy-momentum tensor is given by

$$T_g^{\mu\nu} = pg^{\nu\mu} + (\epsilon+p)U^\nu U^\mu + F_\sigma^\mu F^{\nu\sigma} - \frac{1}{4}g^{\mu\nu}F^{\lambda\kappa}F_{\lambda\kappa} \, ,$$

where $g^{\mu\nu}$ and $F^{\nu\mu}$ are the components of the space-time metric and of the stress tensor of the electromagnetic field, respectivety. In the case of the metric satisfy $g_{\mu\nu} = 0$ for $\mu \neq \nu$, we have $h_0 = \sqrt{-g_{00}}$, $h_1 = \sqrt{g_{11}}$, $h_2 = \sqrt{g_{22}}$ and $h_3 = \sqrt{g_{33}}$.

Equations (1)-(4) are rewritten to have a similar formulation to a conservation law, but with an additional source term. The variables are represented by the following vector

$$\mathbf{u} = \begin{pmatrix} D & P_1 & P_2 & P_3 & \epsilon & B_1 & B_2 & B_3 \end{pmatrix}^T;$$

in which D is density; P_1, P_2 and P_3 are the components of the momentum; ϵ internal energy; B_1, B_2 and B_3 componets of magnetic field.

The interest in rewriting (1)-(4) for the conservation laws format arises from the use of finite volume methods for obtaining approximate solutions. This formulation was initially developed by Koide, Kudoh and Shibata [16] and other formulations are discussed in [9].

In this formulation, the components of the vectors $\mathbf{v}$ of velocity, $\mathbf{B}$ of magnetic field and $\mathbf{E}$ of electric field, in fiducial coordinates, are defined by

$$v_i = \frac{c}{\gamma} h_i U^i \, , \qquad (5)$$
$$B_i = \epsilon_{ijk} \frac{h_i}{J} F^{jk} \, , \qquad (6)$$
$$E_i = \frac{1}{h_0 h_i} F^{0i} \, , \qquad (7)$$

where $i, j, k = 1, 2, 3$, γ is the Lorentz factor and $J = h_1 h_2 h_3$ is the Jacobian.

The conserved quatities are given by

$$D = \gamma\rho \, , \qquad (8)$$
$$\epsilon = (e + p)\gamma^2 - p - Dc^2 + \frac{1}{2}\left(B^2 + \frac{E^2}{c^2}\right) \, , \qquad (9)$$
$$\mathbf{P} = \frac{1}{c^2}\left[(e + p)\gamma^2\mathbf{v} + \mathbf{E} \times \mathbf{B}\right] \, , \qquad (10)$$

and energy-momentum tensor,

$$T = p\mathbf{I} + \frac{1}{c^2}(e + p)\gamma^2\mathbf{vv} - \mathbf{BB} - \frac{1}{c^2}\mathbf{EE} + \frac{1}{2}\left(B^2 + \frac{E^2}{c^2}\right)\mathbf{I} \, , \qquad (11)$$

with the componens being

$$T^{ij} = h_i h_j T_g^{ij} \, , \, i, j = 1, 2, 3 \, .$$

The magnetic and electric field are normalized by the magnetic permeability μ, that is,

$$\mathbf{B} = \frac{\mathbf{B}_*}{\sqrt{\mu}} \quad \text{e} \quad \mathbf{E} = \frac{\mathbf{E}_*}{\sqrt{\mu}} \, ,$$

where the quantities with asterisk are standard units of the international system.

In addition to the assumptions and equations presented in this section, we consider the problem under study with axial symmetry, that is, the problem has no variation with respect to azimuthal variable ϕ. In this case the problem is two-dimensional in space, so the spatial variables are: radial r and polar θ. However, with $x_1 = r$, $x_2 = \theta$ and the hypothesis of axial symmetry, the equations are reduced to

World Academy of Science, Engineering and Technology
International Journal of Mathematical and Computational Sciences
Vol:9, No:1, 2015

Mass Equation:

$$\frac{\partial D}{\partial t} = -\frac{1}{J}\left\{\frac{\partial}{\partial x^1}\left(h_0 h_2 h_3 D v_1\right) + \frac{\partial}{\partial x^2}\left(h_0 h_3 h_1 D v_2\right)\right\}$$
(12)

Motion Equations:

$$\frac{\partial P_1}{\partial t} = -\frac{1}{J}\left\{\frac{\partial}{\partial x^1}\left(h_0 h_2 h_3 T^{11}\right) + \frac{\partial}{\partial x^2}\left(h_0 h_3 h_1 T^{12}\right)\right\} + S_2$$
(13)

$$\frac{\partial P_2}{\partial t} = -\frac{1}{J}\left\{\frac{\partial}{\partial x^1}\left(h_0 h_2 h_3 T^{21}\right) + \frac{\partial}{\partial x^2}\left(h_0 h_3 h_1 T^{22}\right)\right\} + S_3$$
(14)

$$\frac{\partial P_3}{\partial t} = -\frac{1}{J}\left\{\frac{\partial}{\partial x^1}\left(h_0 h_2 h_3 T^{31}\right) + \frac{\partial}{\partial x^2}\left(h_0 h_3 h_1 T^{32}\right)\right\} + S_4$$
(15)

Energy Equation:

$$\frac{\partial \epsilon}{\partial t} = -\frac{1}{J}\left\{\frac{\partial}{\partial x^1}\left[h_0 h_2 h_3\left(P_1 - D v_1\right)\right]\right\} +$$
$$-\frac{1}{J}\left\{\frac{\partial}{\partial x^2}\left[h_0 h_3 h_1\left(P_2 - D v_2\right)\right]\right\} + S_5$$
(16)

Equations of Magnetic Field:

$$\frac{\partial B_1}{\partial t} = -\frac{h_1}{J}\left\{\frac{\partial}{\partial x^2}\left(h_0 h_3 E_3\right)\right\}$$
(17)

$$\frac{\partial B_2}{\partial t} = -\frac{h_2}{J}\left\{-\frac{\partial}{\partial x^1}\left(h_0 h_3 E_3\right)\right\}$$
(18)

$$\frac{\partial B_3}{\partial t} = -\frac{h_3}{J}\left\{\frac{\partial}{\partial x^1}\left(h_0 h_2 E_2\right) - \frac{\partial}{\partial x^2}\left(h_0 h_1 E_1\right)\right\}$$
(19)

Source Terms:

$$S_2 = h_0\left\{(\epsilon + D)G_{01} + G_{12}T^{21} + G_{13}T^{31}\right\} +$$
$$-h_0\left\{G_{21}T^{22} + G_{31}T^{33}\right\}$$
(20)

$$S_3 = h_0\left\{(\epsilon + D)G_{02} + G_{23}T^{32} + G_{21}T^{12} +\right\}$$
$$-h_0\left\{G_{32}T^{33} + G_{12}T^{11}\right\}$$
(21)

$$S_4 = h_0\left\{(\epsilon + D)G_{03} + G_{31}T^{13} + G_{32}T^{23}\right\} +$$
$$-h_0\left\{G_{13}T^{11} + G_{23}T^{22}\right\}$$
(22)

$$S_5 = h_0\left\{G_{01}P_1 + G_{02}P_2 + G_{03}P_3\right\}$$
(23)

On (1)-(4), gravitation is added through the source term and the metric components, h_μ, $\mu = 0, 1, 2, 3$, are represented by componets $G_{\mu\nu}$ defined by

$$G_{\mu\nu} = -\frac{1}{h_\mu h_\nu}\left(\frac{\partial h_\mu}{\partial x^\nu}\right),$$
(24)

where $\mu, \nu = 0, 1, 2, 3$.

The fluid is considered free of electromagnetic forces and this restriction is known as *frozen-in* condition, given by the following relationship,

$$\mathbf{E} = -\mathbf{v} \times \mathbf{B}.$$
(25)

We note that the spatial and temporal derivatives are separated, which defines the formalism $(2+1)$ of equations GRMHD. As the intention is to use these equations to model the formation of jets, initially the model should begin from an accretion disk rotation and in fall with respect to a central compact object, which on this work it was considered a Schwarzschild black hole represented by Schwarzschild metric.

B. Schwarzschild Metric

The problem proposed of relativistic jets is modeled by flow of magnetic fluid in the Schwarzschild spacetime whose metric is static. This means that the central black hole is responsible for all gravitation involved on the problem. Therefore, on this model, the fluid has no self-gravitation and so the gravitation is fully pre-determined by the following Schwarzschild metric,

$$ds^2 = -\alpha^2 dt^2 + \frac{1}{\alpha^2}dr^2 + r^2 d\theta^2 + r^2\sin^2\theta d\phi^2$$
(26)

in which

$$\alpha = \sqrt{1 - \frac{r_s}{r}}, \quad \text{with} \quad c = G = 1, \quad M = \frac{1}{2}r_s \,(BH\ mass),$$

$$h_0 = \alpha, \quad h_1 = \frac{1}{\alpha}, \quad h_2 = r, \quad h_3 = r\sin\theta,$$

where α is the lapse function and r_s is the Schwarzschild radius used as reference unit. The constants c and G are the light velocity and universal gravitational constant. The coordinates (t, r, θ, ϕ) are respectively time, the radial coordinate, the azimuthal and polar coordinate.

C. Accretion Disk

Simulations with stable jets formations is obtained through a initial accretion disk whose thickness is geometrically fine [18], [20]. The initial matter of the disk has a rotation velocity on azimuthal direction and this component of the velocity vector coincides with the Keplerian velocity [4], that is,

$$v_\phi = v_K = \frac{c}{\sqrt{2\left(\frac{r}{r_s} - 1\right)}}.$$
(27)

World Academy of Science, Engineering and Technology
International Journal of Mathematical and Computational Sciences
Vol:9, No:1, 2015

The accretion disk is a magnetized fluid, which is initially localized on

$$|\cot\theta| \leq \delta \quad \text{and} \quad r \geq r_D = d_{in}r_s \qquad (28)$$

where $d_{in} > 1$ is the position of the internal edge whose rotation velocity is

$$v_K = \frac{c}{\sqrt{2(d_{in}-1)}} \ .$$

A value studied for the opening of the disk is $\delta = 0.125$, i.e., if θ is the angle with respect to the equator belonging to the interval $]0, \pi/2[$ radians, then $\delta = 0.125$ implies that the disk occupies a sector of one-eighth of the corresponding sector to interval $]0, \pi/2[$. See the simulations of the Section IV.

The magnetosphere that surrounds the system compound of the accretion disk and the black hole is less dense than the fluid that makes up the disc and, initially, it is in falling toward the black hole containing only the radial component of the speed non-zero. Thus, the initial conditions on the density and velocity of matter around the black hole are given by

Density:

$$\rho = \rho_{mag} + \rho_{disk} \qquad (29)$$

where ρ_{mag} is density of fluid in the magnetosphere and ρ_{disk} is disk density. For the delimitation of the disk has been

$$\rho_{disk} = \begin{cases} \kappa_\rho \rho_{mag}, & if \ r > r_D \ and \ |\cot\theta| < \delta \\ 0, & if \ r \leq r_D \ or \ |\cot\theta| \geq \delta \end{cases}, \qquad (30)$$

in which κ_ρ is ratio between disk density and magnetosphere density.

Velocity:

$$(v_r, v_\theta, v_\phi) = \begin{cases} (0, 0, v_K), & if \ r > r_D \ and \ |\cot\theta| < \delta \\ (-v_{mag}, 0, 0), & if \ r \leq r_D \ or \ |\cot\theta| \geq \delta \end{cases} \qquad (31)$$

where v_K is the Keplerian velocity, v_{mag} is the infalling velocity localized in magnetosphere, r_D is the inner edge of the disk and δ is related with opening angle of the disk.

Initially the disk is magnetized and for additional property, we use the solution Wald whose components are given by

Magnetic Field:

$$\begin{cases} B_r = B_0 \cos\theta \\ B_\theta = -\alpha B_0 \sin\theta \\ B_\phi = 0 \end{cases}, \qquad (32)$$

in which $B_0 = \kappa_B\sqrt{\rho_D c^2}$ and ρ_D is the density at the inner edge of the disk [33].

One way to determine v_{mag} is through the following equation [16],

$$\alpha = \frac{H(\gamma^{-2} + \Gamma - 2)}{(\Gamma - 1)\gamma}, \qquad (33)$$

where H is the constant related to the enthalpy of the fluid, Γ is a constant related to the specific heat, α is the lapse function and γ is the Lorentz factor function. Equation (33) ensures that there is a sonic point between the values of γ satisfying the equality. This point separates regions where the fluid has transonic and subsonic speeds, and this property makes accretion disk more realistic [4].

The magnetosphere region has only the radial component of velocity $v_r = -v_{mag}$. Thus, solving (33) by Newton-Raphson method we find values of γ to each α and, therefore v_{mag} is determined for Lorentz factor, that is, $\gamma = 1/\sqrt{1 - \beta^2}$ where $\beta = v_{mag}/c$.

With the assumption that the gas (plasm) is polytropic, that is, $p = \rho^\Gamma$ and that the ratio between density and pressure is given by [4], [16],

$$a = \frac{p}{\rho} = \frac{\Gamma - 1}{\Gamma}\left(\frac{H}{\alpha\gamma} - 1\right)c^2 \ . \qquad (34)$$

This information is sufficient to make the initial setting of the magnetized accretion disk on rotating, surrounded by a magnetosphere, both influenced by the Schwarzschild black hole. However, to determine the expressions found, the GRMHD differential equations that model the temporal evolution of the phenomenon, require an expression that relates density, pressure, magnetic field and energy, that is, it will be required an *equation of state*.

D. Equation of State

The system of algebraic equations which relate the quantities of equations used in formation problems relativistic jets is represented by the following equations

$$x(x+1)\left[\Gamma ax^2 + (2\Gamma a - b)x + \Gamma a - b + d\tfrac{\Gamma}{2}y^2\right]^2 =$$
$$= \left(\Gamma x^2 + 2\Gamma x + 1\right)^2\left[\tau^2(x+1)^2 + 2\sigma y + 2\sigma xy + \beta^2 y^2\right]$$

$$\left[\Gamma(a - \beta^2)x^2 + (2\Gamma a - 2\Gamma\beta^2 - b)x + \Gamma a - b + d - \beta^2\right]y$$
$$+\tfrac{\Gamma}{2}y^2 = \sigma(x+1)(\Gamma x^2 + 2\Gamma x + 1) \ , \qquad (35)$$

where

$$x = \gamma - 1 \ , \ y = \gamma(\mathbf{v}\cdot\mathbf{B}) \ , \ a = D + \epsilon \ , \ b = (\Gamma - 1)D \ ,$$
$$d = (1 - 0,5\Gamma)B^2 \ , \tau = P \ , \ \beta = B \ and \ \sigma = \mathbf{B}\cdot\mathbf{P}.$$

In (35), the values x and y are unknown and the way chosen to solve it was through the Newton-Raphson method [26], [25]. As at each time step, the GRMHD equations require to resolution of such system, thus the initial approach required by the Newton-Raphson method is chosen as the solutions x and y found in the previous time step. Details on the equation of state are in [21] e and initial studies in [27].

World Academy of Science, Engineering and Technology
International Journal of Mathematical and Computational Sciences
Vol:9, No:1, 2015

E. Initial and Boundary Conditions

The initial conditions must model the accretion disk along with the magnetosphere and the central black hole. Thus, we implemented a modular structure in Fortran 90 specifically to deal with such stage, which is the construction of the equations of Sections II-A,B and C.

In the case of boundary conditions on the magnetosphere region between the inner and outer radii, the matter should continue with their dynamic beyond the domain. Therefore, in this region we used radiation conditions.

In outer edge, the disk is fed through matter, thus in this region we applied Rodin condition. To the boundaries $\theta = 0$ e $\theta = \frac{\pi}{2}$, we used mirror symmetry.

These conditions are fundamentals at applied numerical methods to obtain approximate solutions of differential equations.

III. NUMERICAL METHODS

A. Comparisons

We implemented codes of the following methods: Lax-Friedrichs (L-F) without staggered mesh [19]; Lax-Wendroff-Richtmyer (LWR) [19]; Lax-Wendroff-Richtmyer for spatial discretization and Runge-Kutta 3 TVD for temporal discretization (LWR-RK3) [15]; Nessyahu-Tadmor with staggered grid (NT-ST) [23] and Godunov with Riemann Solver of Harten-Lax-Leer (G-HLL) [13], [14]. All these to find approximate solutions of the Euler equations and to compare them. The codes to Euler Equations were written in Octave, executed with *octave version 3.6.4* in Linux/GNU (kernel 3.8.0-30).

The one-dimensional Euler equations are

$$\frac{\partial}{\partial t}\rho + \frac{\partial}{\partial x}\left(\rho v\right) = 0 \text{ (mass equation)} \tag{36}$$

$$\frac{\partial}{\partial t}\rho v + \frac{\partial}{\partial x}\left(\rho v^2 + p\right) = 0 \text{ (motion equation)} \tag{37}$$

$$\frac{\partial}{\partial t}E + \frac{\partial}{\partial x}\left(v\left(E + p\right)\right) = 0 \text{ (energy equation)} \tag{38}$$

where

$$
\begin{array}{ll}
\rho = \rho(x,t) & \text{(mass density of fluid)} \\
v = v(x,t) & \text{(velocity)} \\
p = p(x,t) & \text{(pressure)} \\
E = E(x,t) & \text{(total energy of the fluid)} \\
\epsilon = \epsilon(x,t) & \text{(internal energy)} \\
\gamma & \text{(specific heat of fluid)}
\end{array}
$$

with

$$E = \frac{1}{2}\left(\rho v^2 + \epsilon\right) \quad \text{and} \quad \epsilon = \frac{p}{(\gamma - 1)\rho}.$$

Consider the following initial conditions (known as Woodward & Colella problem [34]):

$$\rho(x,0) = \begin{cases} 1.0 & \text{if } x < 2 \\ 1.0 & \text{if } x > 2 \end{cases}, \quad v(x,0) = \begin{cases} 0.0 & \text{if } x < 2 \\ 0.0 & \text{if } x > 2 \end{cases}$$

and

$$p(x,0) = \begin{cases} 0.01 & \text{if } x < 2 \\ 1,000.00 & \text{if } x > 2 \end{cases}. \tag{39}$$

With $\gamma = 1.4$, $x \in [0,4]$, $\Delta x = 0.005$ and final time $t_f = 0.4$ we obtained the Table I and the Figs. 1-6. For all methods we used $\Delta t = CFL.\Delta x$

TABLE I
INFORMATION ON THE COMPUTATIONAL PERFORMANCE OF EACH NUMERICAL METHOD

Methods	CFL	time steps	CPU time (s)
L-F	0.02	400	4.01
G-HLL	0.02	400	10.06
NT-ST	0.008	1,000	17.37
LWR-RK3($*$)	0.02	400	20.85
LWR ($**$)	0.0001-0.04	-	-

($*$) stable between 0.01 and 0.02, unstable to 0.005 and 0.04.
($**$) unstable method between 0.0001 and 0.04.

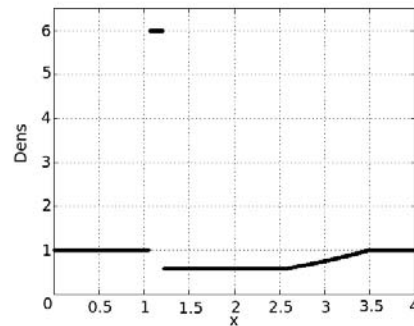

Fig. 1 Density evolution: This graph is the reference exact solution obtained by [32]

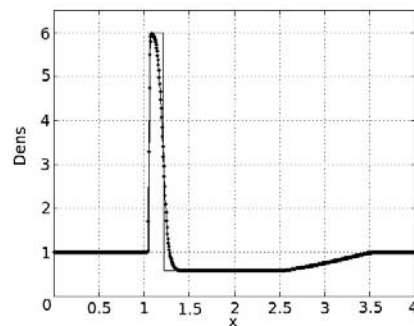
Fig. 2 Density evolution: In this graph we plotted the aproximate solution obtained by Godunov method with Riemann Solver HLL.

The graph of Fig. 3 shows the solution found by the Lax-Friedrichs method. In compared to other methods, the solution obtained at the density showed the dissipative character of the L-F method.

In the Fig. 4, we have the solution obtained by Nessyahu-Tadmor method and this remained less dissipative than L-F method, even needing more iterations when compared to Lax-Friedrichs, see Table I.

World Academy of Science, Engineering and Technology
International Journal of Mathematical and Computational Sciences
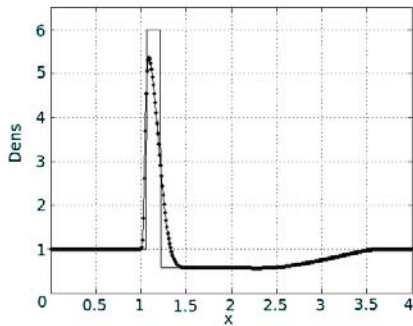Vol:9, No:1, 2015

Fig. 3 Density evolution: The solution obtained by the
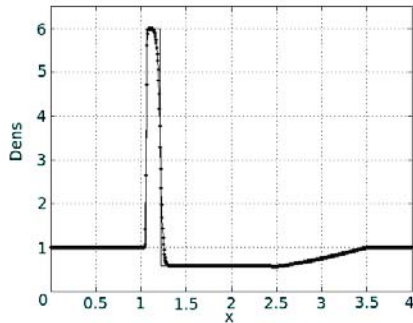Lax-Friedrichs method

Fig. 4 Density evolution: In this graph we have the solution
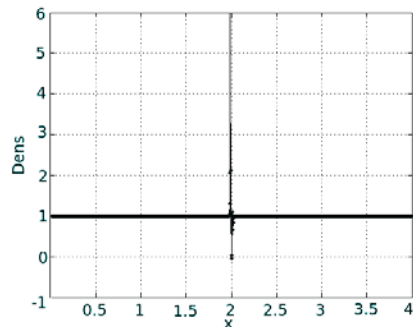obtained by the Nessyahu-Tadmor method

Fig. 5 Density evolution: The solution obtained by the LWR
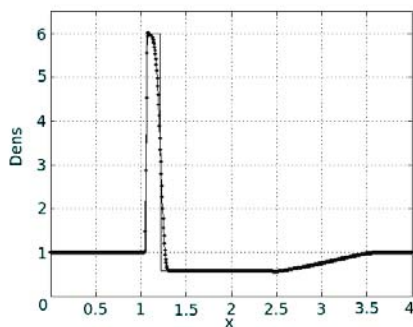method with excessive dispersion (numerical oscillation)

Fig. 6 Density evolution: The solution obtained by
LWR-RK3TVD method

Comparing the methods NT-ST and G-HLL, Figs. 2, 4, the approximate solutions have similar behaviors. However, there are differences between the methods. For example, NT-ST method needed CPU time longer than the G-HLL method, see Table I, and G-HLL requires that the eigenvalues of the Jacobian matrix are known (analytically or numerically).

Although the solutions show great similarities, the solutions obtained by the Nessyahu-Tadmor method stood out because it is possible to see a better representation of the peak that appears in the density-graph and a better representation of internal energy graph.

The solutions obtained by the Lax-Wendroff's methods are in Figs. 5 and 6. In the graphs of Fig. 5, we have the solution obtained by the Lax-Wendroff-Richtmyer method, whose evolution has not reached the final time due to large oscillations (numerical dispersions). In an attempt to stabilize it , we ranged the CFL values from 0.0001 until 0.04, however it was not possible to obtain a stable solutions.

Fig. 5 has plotted the solution to the values $CFL = 0.0001$, $1,200$ iterations and for the final time of 6.10^{-4}, we had an *overflow* with a little more of iterations.

We notice that same the Lax-Wendroff-Richtmyer method being consistent and conditionally stable [30], it was unable to get a stable solution due to spread of large oscillations near the discontinuity of the initial pressure, that were begun from the firsts time steps.

The modifications made on the Lax-Wendroff method through the Runge-Kutta 3 TVD for the temporal discretization were able to control the large initial oscillation and stabilize the numerical solution, see Fig. 6.

The computational cost of these methods are shown in Table I. The Nessyahu-Tadmor method delayed 4.3 times longer to execute the same final time realized by Lax-Friedrichs method and LWR-RK3TVD method spent nearly 4 times more to achieve the developments obtained by the Lax-Friedrichs. On the other hand, Nessyahu-Tadmor was the best method that represented the evolution of the initial discontinuity of pressure and other discontinuities subsequent to initial conditions. Other tests and comparisons between methods are exposed in [11].

With these comparisons we choose to apply the Nessyahu-Tadmor method on (12)-(19). In the next subsection we're presenting the expression of the Nessyahu-Tadmor method and next section IV, we exposed the numerical solutions obtained for a problem of jets formation.

B. Bidimensional Nessyahu-Tadmor Method

By it is a natural extension of the Lax-Friedrichs scheme, Nessyahu-Tadmor method keeps the robustness of the Lax-Friedrichs, providing stable solutions without spurious oscillations and excessive numerical dissipation [23]. This method starts of a law of conservation and considers each finite volume in a staggered mesh. With a stability condition (CFL condition), the method keeps the discontinuities into of the finite volumes and avoids of solvering a Riemann problem at each edge of the finite volumes.

World Academy of Science, Engineering and Technology
International Journal of Mathematical and Computational Sciences
Vol:9, No:1, 2015

we get the **bidimensional Nessyahu-Tadmor method** on staggered mesh,

$$\overline{w}_{i+1/2,j+1/2}^{n+1} = \frac{1}{4}\left(\overline{w}_{i,j}^n + \overline{w}_{i+1,j}^n + \overline{w}_{i,j+1}^n + \overline{w}_{i+1,j+1}^n\right) +$$

$$+ \frac{1}{16}\left[(D_x w_{i,j} - D_x w_{i+1,j}) + (D_x w_{i,j+1} - D_x w_{i+1,j+1})\right] +$$

$$+ \frac{1}{16}\left[(D_y w_{i,j} - D_y w_{i,j+1}) + (D_y w_{i+1,j} - D_y w_{i+1,j+1})\right] +$$

$$- \lambda_x \left[f\left(w_{i+1,j}^{n+1/2}\right) - f\left(w_{i,j}^{n+1/2}\right) - f\left(w_{i+1,j+1}^{n+1/2}\right) + f\left(w_{i,j+1}^{n+1/2}\right)\right]$$

$$- \lambda_y \left[g\left(w_{i,j+1}^{n+1/2}\right) - g\left(w_{i,j}^{n+1/2}\right) - g\left(w_{i+1,j+1}^{n+1/2}\right) + g\left(w_{i+1,j}^{n+1/2}\right)\right] \tag{40}$$

where

$$D_x w_{i,j} = MM\left\{\Delta_x w_{i+1/2,j}^n , \Delta_x w_{i-1/2,j}^n\right\}$$

with

$$\Delta_x w_{i+1/2,j}^n = \overline{w}_{i+1,j}^n - \overline{w}_{i,j}^n$$

and

$$D_y w_{i,j} = MM\left\{\Delta_y w_{i,j+1/2}^n , \Delta_y w_{i,j-1/2}^n\right\}$$

with

$$\Delta_y w_{i,j+1/2}^n = \overline{w}_{i,j+1}^n - \overline{w}_{i,j}^n .$$

For (40) we have

$$\lambda_x = \frac{\Delta t}{2\Delta x} \quad\text{and}\quad \lambda_y = \frac{\Delta t}{2\Delta y}.$$

The symbol $MM\{\cdot,\cdot\}$ is the *minmod function* defined by

$$MM\{a,b\} = \frac{1}{2}\left[sign(a) + sign(b)\right]\min\{|a|,|b|\}, \tag{41}$$

with $sign(a)$ being the signal of number a, and the expressions with $n+1/2$ are given by

$$w_{i,j}^{n+1/2} = \overline{w}_{i,j}^n - \frac{\Delta t}{2\Delta x}D_x f_{i,j} - \frac{\Delta t}{2\Delta y}D_y g_{i,j} , \tag{42}$$

with

$$D_x f_{i,j} = MM\{\Delta_x f_{i+1/2,j}, \Delta_x f_{i-1/2,j}\},$$

in which $\Delta_x f_{i+1/2,j} = f_{i+1,j} - f_{i,j}$ and

$$D_y g_{i,j} = MM\{\Delta_y g_{i,j+1/2}, \Delta_y g_{i,j-1/2}\},$$

with $\Delta_y g_{i,j+1/2} = g_{i,j+1} - g_{i,j}$.

Remark, if

$$D_x w = D_y w = D_x f = D_y g = 0,$$

then (40) reduces to **bidimensional Lax-Friedrichs method** on staggered mesh. These methods may also be obtained in a non-staggered mesh [19], [23], [30]. On the (40) and its subsequent definitions, $\overline{w}_{i,j}^n$ represents the approximate solution on time step n, at each (x_i, y_j) point of the discretized mesh.

Following these same ideas, we applied the

Nessyahu-Tadmor method to discretize and implement the GRMHD equations described in subsection II-A. In the next subsection, we will show as adding source term.

C. Decomposition of Source Term

The implemented (12)-(19) are the following form,

$$u_t + f(u)_x + g(u)_y = s(u) .$$

Before applying the Nessyahu-Tadmor method, we separate the Partial Differential Equation (PDE) with source term at a PED homogeneous and an Ordinary Differential Equation (ODE) involving the source term. Thus, between the time t_n and t_{n+1} we have the following problems

$$\begin{cases} u_t + f(u)_x + g(u)_y = 0 \\ u(x,y,t_n) = u^n \end{cases} \Rightarrow \overline{u}^{n+1} \tag{43}$$

and

$$\begin{cases} \dfrac{du}{dt} = s(u) \\ u(x,y,t_n) = \overline{u}^n \end{cases} \Rightarrow u^{n+1} . \tag{44}$$

Therefore, to perform a time step from t_n to t_{n+1}, we obtain an approximate solution to (43) and use this solution as the initial condition of the ODE.

Equation (43) is solved by Nessyahu-Tadmor method [2] and the solution is updated solving (44) for a four-stage Runge-Kutta method [25].

IV. JETS SIMULATIONS

In the problem of formation of relativistic jets, we implemented the two-dimensional Nessyahu-Tadmor method without dimensional separation, described in section III-B, through of modular structure of the Fortran 90. We used Euler method of four stages to solve the ODE that adds the source term III-C. The code was written completely in Fortran 90 without the use of packages ready and it is described in [11].

With Nessyahu-Tadmor method we got simulations of formation jets since its accretion disk until the ejection of matter. We obtain simulations without excessive dissipation nor, spurious oscillations until the jet reach 14 times the Schwarzschild radius without using additional techniques computational. Furthermore, we could observe the formation of substructures jet and for this we executed the code in a simple computer. The values used were:

- **Spatial domain:** $[1,1 \quad 20] \times [0,\pi/2]$, that is $r \in [1,1 \quad 20]$ and $\theta \in [0,\pi/2]$ radians;
- **Subintervals:** 630×630, thus $\Delta r = 18,9/630$ and $\Delta\theta = \pi/1260$;
- **Temporal increment:** $\Delta t = 401 \times 0.005 min\{\Delta r, \Delta\theta\}$;
- **Constants:** constant related with specific heat $\Gamma = 5/3$ and enthalpy $H = 1,3$;
- **Opening of disk:** $\delta = 0.125$, that is, $\theta = \cot^{-1}\delta$;
- **Density disk:** 401 times greater than the density of the magnetosphere;
- **Inner edge of disk:** $r_D = 3r_S$, three times the black hole radius;

World Academy of Science, Engineering and Technology
International Journal of Mathematical and Computational Sciences
Vol:9, No:1, 2015

In this case, we were decided to normalize initial data with respect to the value of 401 in order to make with that method works with lower numerical values. This normalization is called the scale factor and can be found in numerical methods applied on dynamic fluids [32]. For a better view of the graphs we use the logarithm to base 10 to the values of density, pressure and total energy. On Figures we have the $z\ axis$ divided by Schwarzschild radius ($\bar{z} = z/r_S$) and horizontal axis is the radius divided by r_S ($\bar{r} = r/r_S$), however the axes are dimensionless quantities.

The following we have the initial graphs, Figs. 7, 8, 9, 10 and 11.
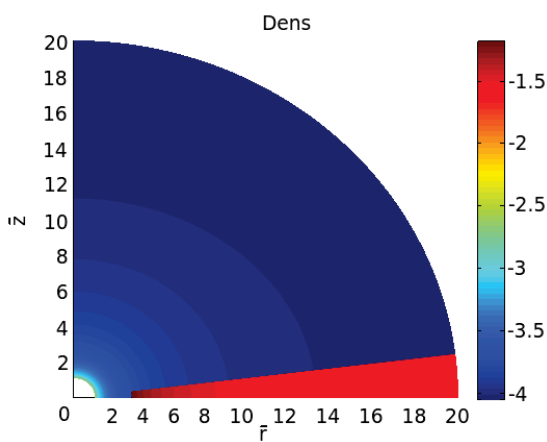
Fig. 7 We have the graph of the initial condition of the density
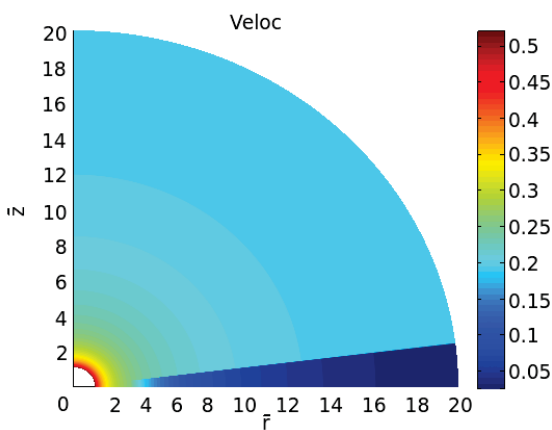
Fig. 8 In this graph we plotted the magnitude initial of the velocity

In these examples the reference unit is the radius of the black hole (BH) and in the graphs, each unit in the vertical and horizontal axes corresponds to the reference unit. The BH is centered at the origin of the graphics and its radius is exactly unity.

The Figs. 12-15 show the temporal evolution of the density. Initially, we have only the accretion disk with rotation surrounding of black hole, with the vertical axis of rotation, and magnetosphere in falling toward the black
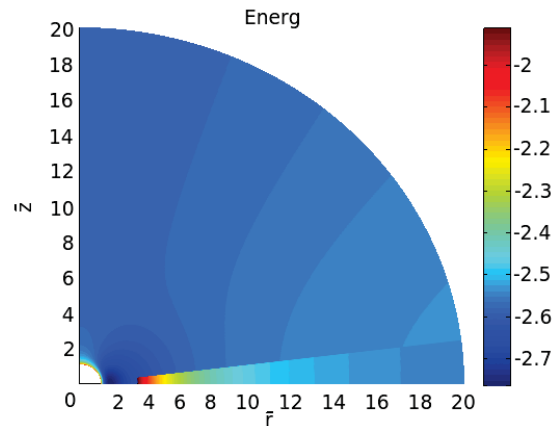

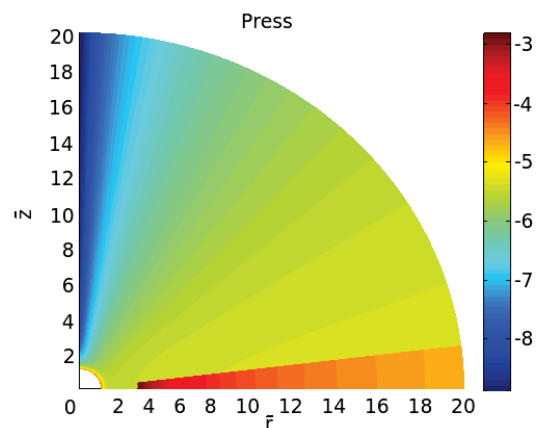Fig. 9 The graph shows the initial total energy

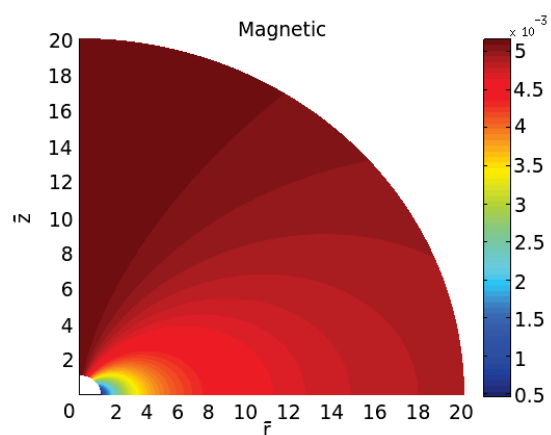Fig. 10 Initial condition of the magnitude of the pressure

Fig. 11 Initial condition of the magnitude of the magnetic field

World Academy of Science, Engineering and Technology
International Journal of Mathematical and Computational Sciences
Vol:9, No:1, 2015

hole. Then the simulation passes by the transition between accretion and ejection, from that moment realizes the ejection of matter in the form of collimated jet along the vertical axis. Finally, the jet extends to the distance of 14 times the radius of the central hole black.

Within the jet stands out the formation of substructures, see Fig. 15. These substructures are compatible with the existing literature on jets [7], [20].
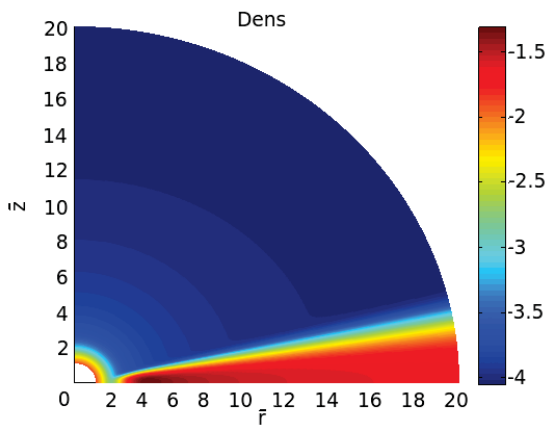
Fig. 12 Density: Numerical solution after 500 iterations

Fig. 13 Density: Numerical solution after 1,000 iterations

Figs. 16-19 show the temporal evolution of total energy. By observing these figures, we noticed a structure is being formed in the accretion disk on the horizontal axis between the values of 2 and 3. This substructure is not permanent and on Fig. 19 notes its disappearance. In connection with the numerical solutions of the total energy also perceives such substructure.

However, we managed to achieve objective of this work to obtain stable approximate solutions for the formation of relativistic jets from the accretion disk to the ejection of matter. Also, we made videos of the approximate solutions of each quantity. In the next section, we will show the conclusions this paper.
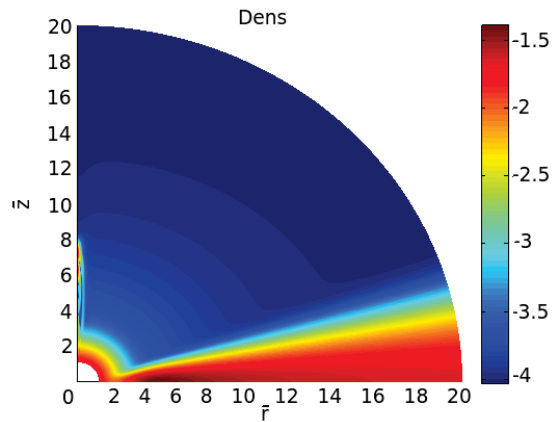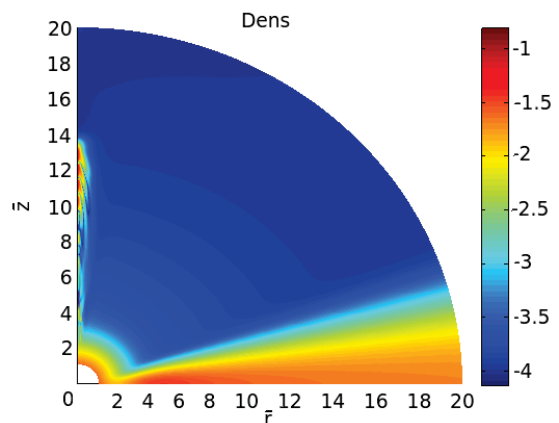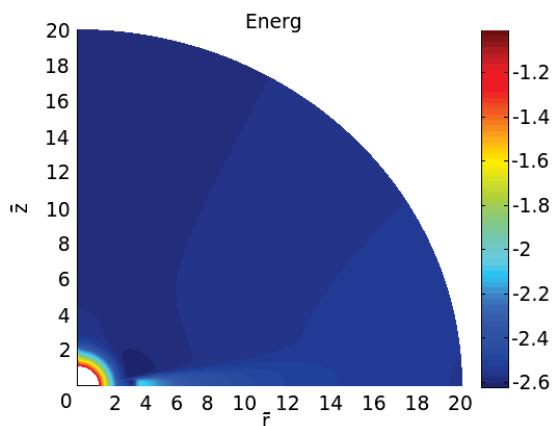

Fig. 14 Density: Numerical solution after 1,500 iterations

Fig. 15 Density: Numerical solution after 2,000 iterations

Fig. 16 Total energy: Numerical solution after 500 iterations

World Academy of Science, Engineering and Technology
International Journal of Mathematical and Computational Sciences
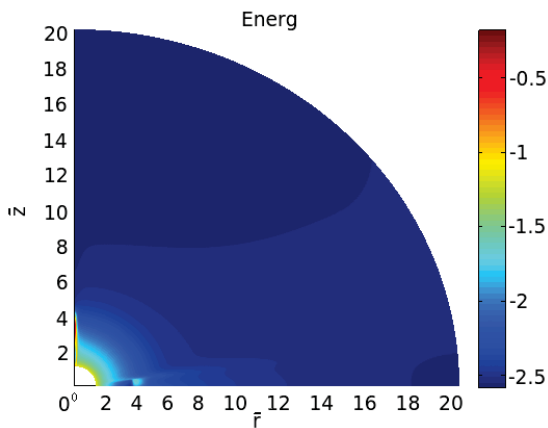Vol:9, No:1, 2015

Fig. 17 Total energy: Numerical solution after 1,000 iterations
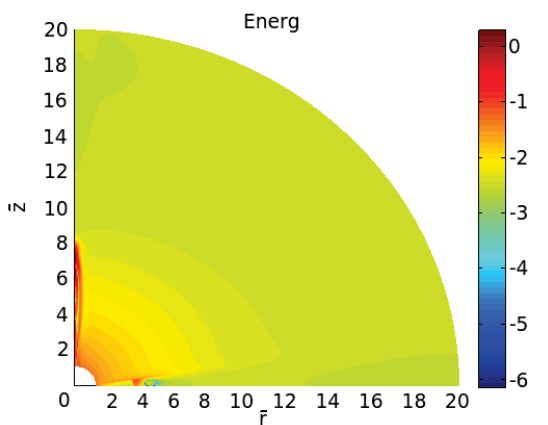

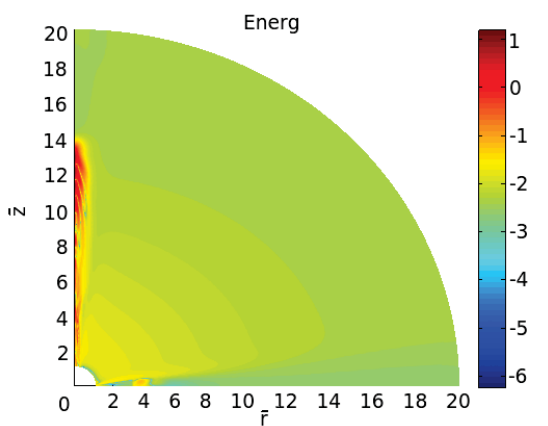Fig. 18 Total energy: Numerical solution after 1,500 iterations

Fig. 19 Total energy: Numerical solution after 2,000 iterations

V. CONCLUSION

This paper we implemented methods Finite Volume Centered , namely: Lax-Friedrichs and Nessyahu-Tadmor applied to problems of formation of relativistic jets from the fall of an accretion disk, rotating around a black hole central (BH) given by the Schwarzschild metric,until the ejection of fluid by the BH poles.

We model this problem through the equations GRMHD, rewritten by Koide et al. formalism [17], with axial symmetry and gravitation predetermined by Schwarzschild metric.

Before for all, we investigated the methods Lax-Friedrichs, Lax-Wendroff's, Godunov and Nessyahu-Tadmor applied to a test problem of the Euler equations.

With the application of two-dimensional Nessyahu-Tadmor method achieved the main objective of this work, because we got simulations that goes through the transition between accretion and ejection without spurious oscillations and excessive numerical dissipation, thus we obtained simulations that are more detailed. In the simulated example, the jet was formed on the poloidal region of the BH and remained stable until it reaches 14 times the radius of the central black hole, a record to this kind of simulations.

With the new code , we could also simulate the formation of substructures that appear in both on the disk and on the jet. Such substructures show the good performance of Nessyahu-Tadmor method by applying it in GRMHD equations with axial symmetry. We made all this into a simple personal computer, which shows the potential of the development of this code to the study of more complete systems and a future parallelism of the code.

Given the performance of the new code, the next step is to exploit it on other Astrophysics examples and to add the third spatial dimension. To this, an important step is to parallelize the code. Finally, we intent of making it available for that other researchers also contribute to the development of the code and expand its applicability.

The continuity of this work can follow to some of the following issues: exploring the Nessyahu-Tadmor method in other astrophysical problems; add an option to run the code in three spatial dimensions; adapt the problem to the Kerr metric; among others.

REFERENCES

[1] P. Anninos, P. C. Fragile, J. D. Salmonson, *Cosmos++ : Relativistic Magnetohydrodynamics on Unstructured Grids with Local Adaptive Refinement*, Astrophys. J., 635 (2005) 7-23.
[2] J. Balbás, E. Tadmor, C.-C. Wu,*Non-oscillatory central schemes for one- and two-dimensional MHD equations: I*, J. Comput. Phys., 201 (2004) pp. 261-285.
[3] V. S. Beskin, *Magnetohydrodynamic models of astrophysical jets*. Phys. Uspekhi, 53 (2010) 1199-1233.
[4] V. S. Beskin, *MHD flows in compact astrophysical objects*, Springer, Heidelberg, 2010.
[5] COCONUT/COCOA.
[6] L. Del Zanna, et al., *ECHO: an Eulerian Conservative High Order scheme for general relativistic magnetohydrodynamics and magnetodynamics*, Astron. Astrophys., 473 (2007) 11-30.
[7] S. S. Doeleman, et al., *Jet-Launching Structure Resolved Near the Supermassive Black Hole in M87*, Science, 338 (2012) 255-258.

World Academy of Science, Engineering and Technology
International Journal of Mathematical and Computational Sciences
Vol:9, No:1, 2015

[8]   H. Falcke, F. W. Hehl, *The Galactic Black Hole - Lectures on general relativity and astrophysics*, IOP, London, 2003.

[9]   J. A. Font, *Numerical Hydrodynamics and Magnetohydrodynamics in General Relativity*, Living Rev. Relativity, 11 (2008).

[10] C. F. Gammie, J. C. McKinney, G. Toth, *HARM: A numerical scheme for general relativistic magnetohydrodynamics*, Astrophys. J., 589 (2003) 444–457.

[11] R. O. Garcia, *Métodos de Volumes Finitos Centrados unsplitting utilizados na obtenção de soluções em Magnetohidrodinâmica: aplicações em discos e jatos*, thesis IMECC/UNICAMP, 2014.

[12] B. Giacomazzo, L. Rezzolla, *WhiskyMHD: a new numerical code for general relativistic magnetohydrodynamics*, Class. Quantum Grav., 24 (2007) S235-S255, 2007.

[13] S. K. Godunov, *A Finite Difference Method for the Computation of Discontinuous Solutions of the Equations of Fluid Dynamics*, Mat. Sb., 47 (1959) 357-393.

[14] A. Harten, P. D. Lax, B. van Leer, *On Upstream Differencing and Godunov-Type Schemes for Hyperbolic Conservation Laws*, SIAM Review, 25 (1983) 35-61. 1983.

[15] W. Hundsdorfer, J. G. Verwer, Numerical Solution of Time-Dependent Advection-Diffusion-Rection Equations, Springer, New York, 2003.

[16] S. Koide, K. Shibata, T. Kudoh, *Relativistic Jet Formation from Black Hole Magnetized Accretion Disk: Method, Test and Applications of a General Relativistic Magnetohydrodynamic Numerical Code*, Astrophys. J., 522 (1999) 727-752.

[17] S. Koide, *General relativistic plasmas around rotating black holes.* Procedings IAU Symposium, 275 (2011).

[18] S. S. Komissarov, et al., *Magnetic acceleration of ultra-relativistic jets in gamma-ray burst sources*, Mon. Not. R. Astron. Soc., 394 (2009) 1182-1212.

[19] R. J. Leveque, *Finite Volume Methods for Hyperbolic Problems*, Cambridge University Press, New York, 2002.

[20] J. C. McKinney, R. D. Blandford, *Stability of relativistic jets from rotating, accreting black holes via fully three-dimensional magnetohydrodynamic simulations*, Mon. Not. R. Astron. Soc., 394 (2009) L126-L30.

[21] A. Mignone, J. C. McKinney, *Equation of state in relativistic magnetohydrodynamics: variable versus constant adiabatic index*, Mon. Not. R. Astron. Soc., 378 (2007) 1118-1130.

[22] P. Mösta, et al., *GRHydro: A new open source general-relativistic magnetohydrodynamics code for the Einstein Toolkit*, Class. Quantum Grav., 31 (2014).

[23] H. Nessyahu, E. Tadmor, *Non-Oscillatory Central Differencing for Hyperbolic Conservation Laws*, J. Comput. Phys., 87 (1990) 408-463.

[24] K. -I. Nishikawa, et al., *A General Relativistic Magnetohydrodynamic Simulation of Jet Formation*, Astrophys. J., 625 (2005) 60-71.

[25] W. H. Press, et al., *Numerical Recipes in Fortran 90*. Cambridge University Press, Second Edtion, United States of American, 1997.

[26] M. J. D. Powell, *Approximation theory and methods*, Cambridge University Press, Cambridge, 2001.

[27] V. Schneider, et al., *New Algorithms for Ultra-relativistic Numerical Hydrodynamics*, J. Comp. Phys., vol. 105, n. 1, pp. 92-107, 1993.

[28] S. L. Shapiro, S. A. Teukolsky, *Black Holes, White Dwarfs and Neutron Stars - The Physics of Compact Objects*, John Wiley & Sons, New York, 1983.

[29] A. Tchekhovskoy, J. C. McKinney, R. Narayan, *WHAM: a WENO-based general relativistic numerical scheme – I. Hydrodynamics*, Mon. Not. R. Astron. Soc., 379 (2007) 469–497.

[30] J. W. Thomas, Numerical Partial Differential Equations: Finite Difference Methods, Springer, New York, 1995.

[31] K. S. Thorne, R. H. Price, D. A. MacDonald, *Black Holes: The Membrane Paradigm*, Yale University Press, New Haven, 1986.

[32] E. F. Toro, Riemann Solvers and Numerical Methods for Fluid Dynamics - A Practical Introduction, third edition, Springer, Germany, 2009.

[33] R. M. Wald, *Black Hole in an uniform magnetic field*, Phys. Rev. D, 10 (1974) 16-80.

[34] P. Woodward, P. Colella, *The Numerical Simulation of Two-Dimensional Fluid Flow with Strong Shocks*, J. Comput. Phys., 54 (1984) 115-173.

Raphael de Oliveira Garcia I am Ph.D. in Applied Mathematics with emphasis in numerical method to PDEs by the University of Campinas/Brazil (Universidade Estadual de Campinas - UNICAMP) and nowadays I work on Department of Applied Mathematics of same University. I graduated in Physics by the Paulista State University (Universidade Estadual Paulista - UNESP) and my interest areas are: numerical method to PDEs, fluid dynamics, astrophysics and scientific computation.

Samuel Rocha de Oliveira holds a BS in Physics from the University of Brasilia (1983), Master in Theoretical Physics from the University of Brasília (1986) and Ph.D. in Physics - University Of Texas At Austin (1992). He is currently Professor Full Professor at the State University of Campinas in Applied Mathematics department. Has research in Physics - Mathematics, acting on the following topics: general relativity, gravitation, black holes, numerical relativity, computational science, astrophysics, partial differential equations and gauge theories. Has also worked in the area of Teaching Mathematics and Science Communication, on the following topics: teaching resources, learning objects, learning mathematics in digital multimedia, production of audio and video programs.